Contribution of transient receptor potential channels to the control of GABA release from dendrites

Thomas Munsch*, Marc Freichel[†], Veit Flockerzi[†], and Hans-Christian Pape*[‡]

*Institut für Physiologie, Medizinische Fakultät, Otto-von-Guericke Universität, Leipzigerstrasse 44, D-39120 Magdeburg, Germany; and [†]Institut für Pharmakologie und Toxikologie, Universität des Saarlandes, D-66421 Homburg Saar, Germany

Neuronal dendrites have been shown to actively contribute to synaptic information transfer through the Ca^{2+}-dependent release of neurotransmitter, although the underlying mechanisms remain elusive. This study shows that the increase in dendritic γ-aminobutyric acid (GABA) release from thalamic interneurons mediated by the activation of 5-hydroxytryptamine type 2 receptors requires Ca^{2+} entry that does not involve Ca^{2+} release nor voltage-gated Ca^{2+} channels in the plasma membrane but that is critically dependent on the transient receptor potential (TRP) protein TRPC4. These data ascribe a functional role of agonist-activated TRP channels to the release of transmitters from dendrites, thereby indicating a principle underlying synaptic interactions in the brain.

A prominent example of dendrodendritic interactions is found in the dorsal lateral geniculate nucleus (LGNd), the main thalamic station of the primary visual pathway, where thalamocortical relay cells receive γ-aminobutyric acid (GABA)-ergic input via two types of synaptic terminals (1). One type is the F1 terminal, which originates from axons of local interneurons or reticular thalamic neurons. The other is the F2 terminal, which derives from dendrites of interneurons, is typically situated within a glomerular neuropil, and is both postsynaptic to retinal afferents and presynaptic to relay cells. The release of GABA from F2 terminals is modulated by extrathalamic input systems acting on metabotropic receptors, as has been shown recently for the glutamatergic and cholinergic systems (2, 3), although the underlying mechanisms remain unknown. In the present study, we have investigated the mechanisms underlying the control of GABA release from the interneuronal dendrites, focusing on serotonin (5-hydroxytryptamine, 5-HT) and glutamate acting on metabotropic receptors, which are related to fibers arising from the dorsal raphé nucleus and to corticofugal fibers, respectively, and are thought to control thalamocortical transmission during the sleep/waking cycle (4, 5). Because the release of GABA from F2 terminals has been found to occur in a Ca^{2+}-dependent manner (2, 3), we have paid particular attention to the involved Ca^{2+} pathways.

Materials and Methods

Tissue Preparation. Thalamic slices were prepared from juvenile postnatal day (P) 12–P18 Long–Evans rats or juvenile (P14–P25) wild-type 129/SvJ and mice deficient in the transient receptor potential (TRP) protein TRPC4, which were back-crossed into the 129/SvJ genetic background for five generations (6). After anesthesia with fluothane, animals were decapitated, and a block of tissue containing LGN and ventrobasal complex was rapidly removed and placed in chilled (2–4°C), oxygenated slicing solution (pH 7.35, with NaOH) containing the following (in mM): sucrose, 195; glucose, 11; Pipes, 20; KCl, 2.5; $MgSO_4$, 10; and $CaCl_2$, 0.5. Coronal slices of the thalamus were cut at 300 μm on a vibratome and kept submerged in artificial cerebrospinal fluid (ACSF) (pH 7.35, with 95% O_2/5% CO_2) containing the following (in mM): NaCl, 125; KCl, 2.5; NaH_2PO_4, 1.25; $NaHCO_3$, 22–26; $MgSO_4$, 2; $CaCl_2$, 2; and glucose, 10.

Electrophysiology. Whole-cell patch-recordings were performed from thalamocortical relay neurons in LGNd and ventrobasal complex. Patch pipettes were filled with the following (in mM; pH 7.25): cesium gluconate, 117; sodium gluconate, 10; CsCl, 13; EGTA, 1; $CaCl_2$, 0.1; Hepes, 10; and $MgCl_2$, 1. During recordings, individual slices were continuously superfused with ACSF (22–25°C). An EPC-9 amplifier (HEKA Electronics, Lambrecht/Pfalz, Germany) operating PULSE software was used for recording spontaneous inhibitory postsynaptic currents (sIPSCs) in voltage-clamp mode. Access resistances ranged from 4 to 10 MΩ. In ACSF containing La^{3+} or Gd^{3+}, HCO_3^- and PO_4^- were replaced by Hepes and Cl^-, respectively. Biocytin labeling (0.5% biocytin) was performed as described previously (7). Morphological analyses were done in a blind manner, i.e., with no knowledge of the physiological data from the same cells.

Data Analysis. Analysis of sIPSC activity was performed with PULSEFIT V. 8.01 software (HEKA Electronics). The membrane current variance (σ^2) was calculated off-line for consecutive 10-s intervals from current traces filtered at 1 kHz. IPSCs were detected by using MINIANALYSIS (Jaejin Software, Leonia, NJ). Cumulative histograms without bins were calculated within time periods of equal duration (3 min) before and after addition of 5-HT. Data are presented as means ± SEM. Comparisons were made with Student's paired t test or with a nonparametric test (Mann–Whitney, two-tailed) as indicated. P values of <0.01 were considered statistically significant.

RNA Expression. Neurons were isolated from rat LGNd slices (P12–P18) through enzymatic dissociation [incubation for 60–90 min at room temperature in 1 mg/ml trypsin type XI (Sigma), followed by trituration with fire-polished, silicone-coated Pasteur pipettes], and interneurons were identified as described previously (8). More than 180 interneurons were harvested by using ACFS (lacking $MgSO_4$)-filled pipettes, collected in 0.2-ml thin-walled PCR tubes (10 cells in 15 to 20 μl of ACSF per tube), and thawed at 4°C. RT-PCR was performed by using the SuperScript One-Step RT-PCR with Platinum Taq system (Invitrogen). Sense and antisense primers (2.5 μl, 10 μM; see Table 1, which is published as supporting information on the PNAS web site), reaction mix, and SuperScript II RT/Platinum Taq DNA polymerase (Invitrogen) were added as specified by the manufacturer. Reactions (50 μl) were mixed and incubated (50°C for 25 min and 94°C for 2 min). Amplification consisted of 35 cycles of 94°C for 15 s, 60°C for 30 s, and 72°C for 30 s; 5 μl was used for reamplification reactions (30 cycles of 94°C for 30 s,

NEUROSCIENCE

60°C for 30 s, and 72°C for 30 s) with *Taq* DNA polymerase and primer combinations (Table 2, which is published as supporting information on the PNAS web site). PCR products (15–40 μl) were analyzed on 2% agarose gels containing 0.5 μg/ml ethidium bromide and on 7% polyacrylamide gels stained after electrophoresis with ethidium bromide. Controls included (*i*) reactions in the absence of cells, (*ii*) reactions in the absence of cells but in the presence of genomic DNA prepared from rat liver by using an EZNA Tissue DNA kit II (PEQLAB Biotechnologie, Erlangen, Germany), and (*iii*) RT-PCRs in the presence of (poly)A$^+$ RNA isolated from rat brain that was reverse-transcribed into cDNA by using the SuperScript First-Strand Synthesis system (Invitrogen). Sense and antisense oligodeoxynucleotide primers (Table 1) were derived from different exons to distinguish between RT-PCR-amplified DNA fragments and fragments amplified from genomic DNA. Rat cDNAs were aligned to the protein-coding cDNAs of the respective mouse genes, which bear 95–96% nucleotide sequence identity, and primers were deduced from the rat sequences by assuming an exon organization identical to that in the mouse sequences. The sizes of the DNAs amplified from single cells were as predicted and identical to the sizes of the respective cDNAs amplified by RT-PCR using brain (poly)A$^+$ RNA as template. Amplification of DNA fragments from genomic DNA was obtained only when using primer combinations in which both primers reside on the same exon (see Table 2; primer combinations KO-15/KO-40, KO-44/KO-45, and GAPDH-1/GAPDH-2).

Results

The GABAergic inputs mediated via axonal F1 and dendritic F2 terminals in LGNd relay cells were identified in whole-cell recordings of sIPSCs in rat LGNd slices, as described previously (2, 3). At a holding potential of 0 mV, bath perfusion of 1–100 μM 5-HT resulted in an increase in sIPSCs (Fig. 1 *A*b and *B*b, $n = 46$), as indicated by the increase in membrane current variance (σ^2) (Fig. 1*A*, bottom trace). During action of 1 μM tetrodotoxin (TTX), a significant proportion of the 5-HT-evoked response was preserved (Fig. 1 *A*c and *B*c), suggesting mediation via F2 terminals (2). That the TTX-resistant component of the 5-HT-induced increase in sIPSC activity reflected activity of F2 terminals was corroborated by the following line of evidence. First, effects of 5-HT were occluded by a nearly maximal response to ($\pm$)-1-aminocyclopentane-*trans*-1,3-dicarboxylic acid (t-ACPD) (125 μM; Fig. 1*C*, $n = 9$), which selectively activates metabotropic glutamate receptors (mGluRs) on F2 terminals under these conditions (2, 3), indicating a convergence of the agonist-activated effects on the same downstream mechanism. Further, the pharmacological profile of the mGluR-mediated responses (as illustrated in Fig. 3) resembled that previously described for F2 terminals in rat and cat LGNd (2, 3). Second, addition of 6,7-dinitroquinoxaline-2,3-dione (DNQX) (10 μM) and 2-amino-5-phosphopentanoic acid (AP5) (50 μM) to the bathing solution ($n = 5$) and inclusion of 2 mM GDP-β-S in the pipette solution ($n = 4$) did not affect responses to 5-HT, evidence against indirect polysynaptic effects and postsynaptic effects of the recorded relay cells, respectively. Third, cumulative probability plots of sIPSCs demonstrated a significant increase in frequency, from 3.28 $\pm$ 0.99 Hz to 5.56 $\pm$ 1.16 Hz ($n = 4$) during action of 5-HT, whereas mean amplitudes remained unchanged (28.47 $\pm$ 1.28 pA vs. 26.58 $\pm$ 1.76 pA), indicating a presynaptic site of action (Fig. 1*D*, $n = 4$). Fourth, recordings from relay cells in the ventrobasal complex, which is essentially devoid of local interneurons and therefore also lacks F2 terminals (9), revealed no significant increase in sIPSC activity on application of 5-HT (Fig. 1*E*, $n = 6$). Fifth, the GABA type A (GABA$_A$) antagonist bicuculline (20 μM) completely suppressed sIPSC activity (Fig. 1 *A*d and *B*d, $n = 12$), confirming

GABA$_A$-dependent IPSCs. Finally, morphological analyses of recorded cells after injection of biocytin ($n = 18$) revealed the existence of two different classes of neurons, possessing type I and type II morphology (10, 11). Type II neurons, which are known to receive dendritic (F2) input (2), all displayed TTX-insensitive responses to 5-HT (Fig. 1*G*, mean increase from baseline = 1,030.9 $\pm$ 107.1%, $n = 12$). Type I neurons, which lack dendritic (F2) input (2), in all but one case lacked TTX-insensitive responses to 5-HT (Fig. 1*F*, $n = 6$). In comparison, TTX-sensitive responses to 5-HT were found in all neurons irrespective of the morphological type, corresponding to the existence of axonal (F1) inputs in both type I and type II neurons (2). All subsequent experiments in the rat LGNd focused on neurons with morphological properties indicative of type II, and TTX (1 μM) was continuously present to isolate F2-mediated responses.

The pharmacological profile of the 5-HT-induced response indicated involvement of the 5-HT$_2$ receptor subtype (Fig. 5, which is published as supporting information on the PNAS web site): the 5-HT$_2$ agonist α-methyl-5-HT (αM-5-HT) induced an increase in sIPSC activity, the average amplitude of which exceeded that of 5-HT tested at the same concentration. Of the other 5-HT agonists tested, the 5-HT$_{2C}$ receptor agonist 6-chloro-2-(1-piperazinyl)pyrazine (MK-212) was most effective, whereas the 5-HT$_{2B/2C}$ agonist 1-(3-chlorophenyl)piperazine (mCPP) evoked no detectable response. Also, the selective 5-HT$_4$ agonist RS 67506 only marginally increased sIPSC activity. By contrast, the 5-HT$_1$ agonist 5-carboxamidotryptamine (5-CAT) increased sIPSC activity to 32 $\pm$ 6% ($n = 6$) of that of the control, indicating the contribution of 5-HT$_{1C}$ (renamed to 5-HT$_{2C}$) receptors (12). The 5-HT$_{2A/2C}$ antagonist ketanserin (50 μM) and the less selective 5-HT$_2$/5-HT$_1$ antagonist mianserin (500 μM) considerably reduced the 5-HT-mediated increase in sIPSC activity. 5-HT$_2$ receptors are typically coupled to the phospholipase C (PLC) inositol trisphosphate system. Indeed, pretreatment (>2 h) of LGNd slices with 10 μM 1-O-octadecyl-2-O-methyl-rac-glycero-3-phosphorylcholine (ET-18-OCH$_3$), an inhibitor of phosphatidylinositol-specific PLC (13, 14), abolished 5-HT responsiveness (Fig. 5*D*, $n = 5$), whereas application of the membrane-permeable diacylglycerol analogue 1-oleoyl-2-acetyl-*sn*-glycerol (OAG) (100 μM) had no effect on sIPSC activity (Fig. 6*A*, which is published as supporting information on the PNAS web site, $n = 4$). Superfusion of 100 μM 2-aminoethoxydiphenyl borate (2-APB) resulted in a progressive attenuation and final blockade of the 5-HT-induced increases in sIPSC (Fig. 6*B*, $n = 6$), reflecting an involvement of inositol trisphosphate receptors (15, 16) or a blocking effect on Ca^{2+}-influx pathways (17, 18).

We thus designed the next experimental steps to characterize the source of Ca^{2+} mediating the increase in dendritic GABA output. Inhibitors of the endoplasmic reticulum Ca^{2+} pump, thapsigargin (1 μM, $n = 7$; data not shown) or cyclopiazonic acid (CPA) (20–50 μM, $n = 7$; Fig. 2*A* and *B*), had no significant effect on basal sIPSC activity or responses to 5-HT, suggesting that Ca^{2+} release does not play a major role. Caffeine, known to induce Ca^{2+} release via ryanodine receptors in thalamic relay neurons (19), resulted in a decrease in resting or 5-HT-induced sIPSC activity ($n = 16$) when superfused alone (10 mM) or in combination with a Ca^{2+}-free (0 Ca^{2+}, 200 μM EGTA) bathing medium ($n = 8$; data not shown). As caffeine has been reported to also inhibit GABA$_A$ and inositol trisphosphate receptors (20, 21), we used a Ca^{2+} removal/readdition protocol to further clarify the role of store depletion-sensitive vs. store depletion-insensitive Ca^{2+} influx (22). Readdition of extracellular Ca^{2+} after a 10-min superfusion with Ca^{2+}-free saline and in the continuous presence of CPA led to a small but significant increase in sIPSC activity, 12 $\pm$ 1.9% of the control response (Fig. 2*B*, $n = 7$), indicating a store-dependent component. In
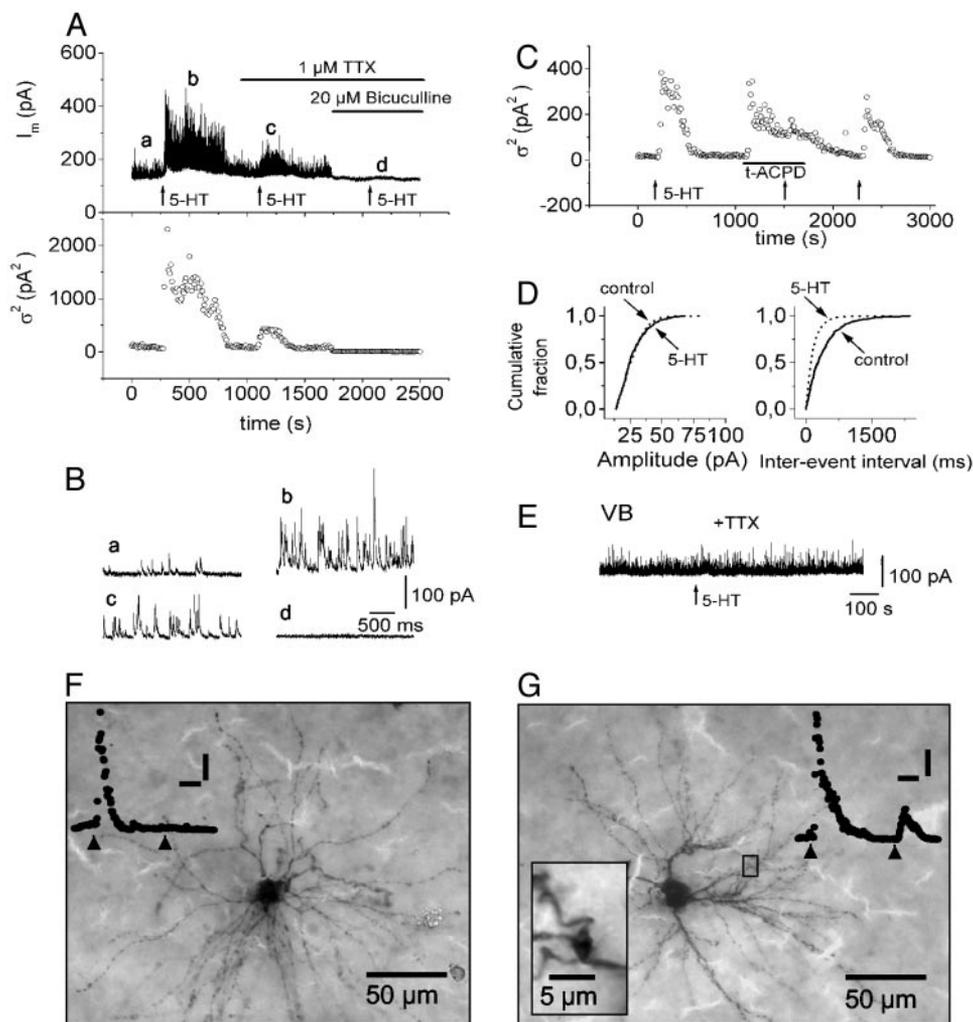
Fig. 1. Effect of 5-HT receptor activation on IPSC activity in rat thalamocortical relay neurons. (*A*) Membrane current (I_m) and membrane current variance (σ^2) of a LGNd relay neuron during activation of 5-HT receptors (application of 5-HT at 10 μM for 1.5 min at times indicated by arrows) in normal ACSF and in the presence of 1 μM TTX and 20 μM bicuculline (indicated by bars). (*B*) Three-second intervals of the continuous current trace in *A* depicted at an expanded time scale at the times indicated (a–d). (*C*) Occlusion of the 5-HT-induced increase in IPSC activity during nearly maximal action of ($\pm$)-1-aminocyclopentane-*trans*-1,3-dicarboxylic acid (t-ACPD) (125 μM). TTX (1 μM) was present throughout the experiment. (*D*) Cumulative probability plots obtained under control conditions and in the presence of 10 μM 5-HT (synaptic events were counted over time periods of 3 min). Recordings were obtained in TTX (1 μM). (*E*) Membrane current of a ventrobasal complex (VB) relay neuron; 100 μM 5-HT was applied (for 1.5 min) at the time indicated by the arrow in the continuous presence of TTX (1 μM). (*F* and *G*) Photomicrographs of biocytin-labeled type I (*F*) and type II (*G*) neurons. Traces show responses of the same cells to 5-HT (application indicated by arrowheads) before (first response) and after (second response) addition of TTX. [Scale bars: 200 s, 200 pA^2 (*F*); and 200 s, 400 pA^2 (*G*).] The neuron in *F* displays radial dendritic morphology consistent with type I morphology and lacks TTX-insensitive responses to 5-HT. The neuron in *G* possesses numerous swellings along dendrites and near branch points typical of type II morphology (*Inset*) and generates TTX-insensitive responses to 5-HT. Note the existence of TTX-sensitive responses in both types of neuron.

comparison, simultaneous readdition of Ca^{2+} and bath-application of 5-HT (100 μM, 1.5 min) strongly increased sIPSC activity (83 $\pm$ 4.5%, $n = 7$), indicating that a store depletion-insensitive mechanism provides the major Ca^{2+} influx (Fig. 2*B*). In support of this view, superfusion of a Ca^{2+}-free solution (0 Ca^{2+}, 200 μM EGTA) reversibly abolished the increase in sIPSC activity as compared with control applications of 5-HT in the presence of extracellular Ca^{2+} in all tested cells (Fig. 2*C*, $n = 9$), and readdition of extracellular Ca^{2+} readily reinstalled responsiveness to 5-HT. Superfusion of Ni^{2+} (500 μM, $n = 5$), Zn^{2+} (100 μM, $n = 6$), La^{3+} (100 μM, $n = 4$), or Gd^{3+} (50 μM, $n = 4$) abolished the 5-HT-induced increase in sIPSC activity (Fig. 7, which is published as supporting information on the PNAS web site), supporting the view that Ca^{2+}-influx is required. To further characterize the Ca^{2+}-influx pathways, dendritic GABA release was unspecifically induced through a high-potassium (20 mM)

bathing solution and compared with that evoked through 5-HT, and a mixture of blockers of voltage-gated Ca^{2+} channels (ω-agatoxin IVA, 1 μM; ω-conotoxin GVIA, 5 μM; calcicludine, 5 μM) was tested. As is illustrated in Fig. 2 *D–F*, the high-potassium-induced activity (1,644.9 $\pm$ 320.9% change from baseline, $n = 6$) was nearly blocked on toxin treatment (71.1 $\pm$ 21.8%, $n = 6$), whereas 5-HT-evoked responses recorded in the same slices remained unaffected (1,347.8 $\pm$ 262.9% vs. 1,389.4 $\pm$ 459.9%, $n = 6$). These data suggested the involvement of a Ca^{2+}-influx pathway distinct from voltage-gated Ca^{2+} channels. Furthermore, La^{3+} at 100 μM ($n = 4$) and Gd^{3+} at 50 μM ($n = 4$) individually caused a slow increase in sIPSC activity and occluded responses to subsequent application of 5-HT (Fig. 7), a property indicative of the recently described actions on heterologously expressed TRPC4 and TRPC5 channels (23, 24).

The TRP superfamily includes a diversity of non-voltage-gated cation channels, some of which are considered candidates

NEUROSCIENCE

<pre>Munsch *et al.*</pre>
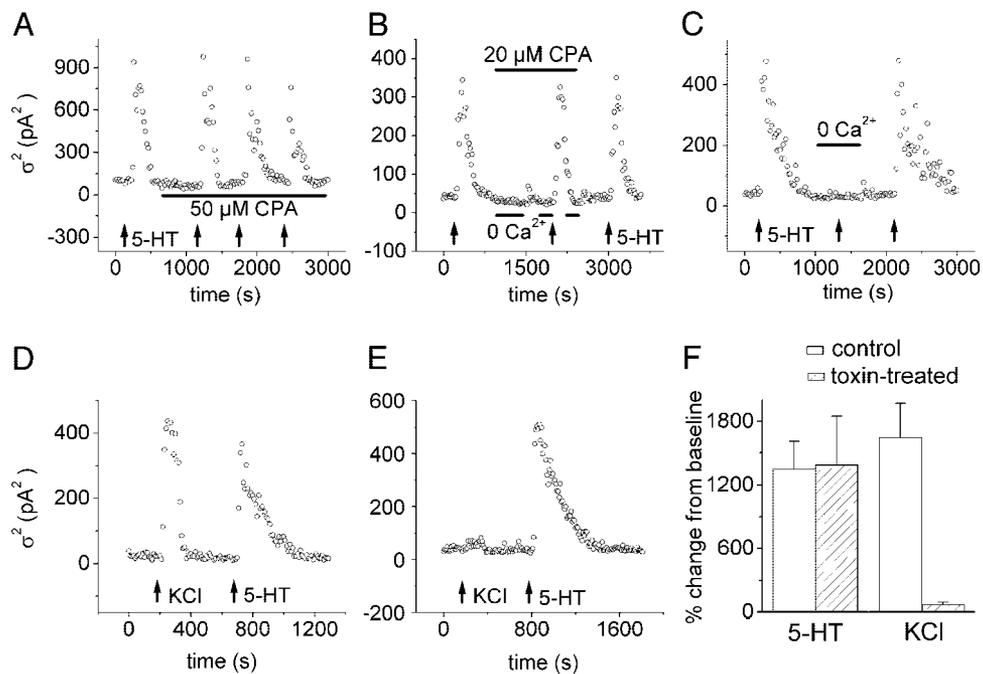
Fig. 2. Source of Ca^{2+} mediating 5-HT$_2$-mediated GABA release. All recordings were obtained from rat LGNd relay neurons in TTX (1 μM), and 5-HT was bath-applied at 100 μM for 1.5 min (indicated by arrows). (*A*) Lack of effect of CPA (50 μM; application period indicated by bar) on basal and 5-HT-induced increases in sIPSC activity. (*B*) Removal and readdition of external Ca^{2+} either without or concomitant with the application of 5-HT and after treatment of the slice with CPA (10 μM). Periods of Ca^{2+} removal and CPA application are indicated by bars. Note that readdition of Ca^{2+} in the presence of CPA evokes a small increase in sIPSC activity and that simultaneous readdition of Ca^{2+} and bath-application of 5-HT strongly increased sIPSC activity. (*C*) Superfusion of the slice with Ca^{2+}-free ACSF (0 Ca^{2+}, 200 μM EGTA; period of application indicated by bar) reversibly blocks 5-HT responsiveness. (*D*) Increase in sIPSCs by superfusion of high-K$^+$- (20 mM KCl) and 100 μM 5-HT-containing ACSF. (*E*) Block of the high K$^+$, but not the 5-HT, evoked response in a slice incubated with ω-agatoxin IVA (1 μM), ω-conotoxin GVIA (5 μM), and calcicludine (5 μM). (*F*) Bar graph summarizing the effects of high K$^+$ (20 mM KCl) and 100 μM 5-HT on sIPSC activity in control and toxin-treated slices. Data represent means ± SEM.

for receptor-operated Ca^{2+} entry, although the exact activation pathways and the functional role are not always clear (25–27). Of particular interest here, the TRPC4 protein is abundantly expressed in the brain and, when expressed, can form homomeric and heteromeric cation channels that are operated through PLC-dependent mechanisms (28, 29). To test the possibility that TRP channels are involved in the F2-mediated GABA release, we performed comparative studies in homozygous knockout mice lacking the TRPC4 subunit (TRPC4$^{-/-}$) (6). Transcript expression levels of other members of the TRPC family are not altered in the brains of these mice (6), indicating that TRPC4 deletion does not affect the expression of other TRPC proteins. All experiments were performed in TTX. Application of 5-HT (100 μM) to LGNd relay cells in wild-type (TRPC4$^{+/+}$) mice caused an increase in sIPSC activity in $\approx$86% of tested cells (25/29), averaging to 521.9 ± 118.9% with respect to baseline levels and with characteristics indistinguishable from those in the rat LGNd (Fig. 3 *A* and *F*). These responses reflected activity of F2 terminals, as was indicated by the finding that the group I mGluR agonist dihydroxyphenylglycol (DHPG) (100 μM) evoked a similar increase in sIPSC activity in all cells tested (mean = 2678.8 ± 928.1%, n = 7). The group II mGluR agonist (*S*)-3-carboxy-4-hydroxyphenylglycine (S3-C4HPG) (250 μM, n = 6) was ineffective (Fig. 3*B*), thereby resembling the pharmacological profile typical of F2-mediated responses in the cat and rat LGNd (2, 3). Furthermore, responses to the 5-HT$_2$ receptor agonist αM-5-HT (100 μM) were occluded by a nearly maximal effect of DHPG (Fig. 3*C*, n = 7). In contrast, in TRPC4$^{-/-}$ mice, 5-HT under the same experimental conditions did not evoke a response in the majority (22/31) of tested cells (Fig. 3 *D* and *E*) and elicited only a residual response in the remainder (9/31) of the cells. The average response amplitude

(Fig. 3*F*, increase in sIPSC from baseline = 32.9 ± 13.6%, n = 31) was significantly smaller than that in TRPC4$^{+/+}$ cells, even when only those cells with residual response were considered (16.0 ± 5.0% with respect to wild-type response, n = 9). Although the variance analysis used in the present study may underestimate the magnitude of responses of a rather slow time course, there was a substantial increase (from 14% to 71%) in the number of cells that were not responsive to 5-HT after knockout of the TRPC4 gene. As a positive control in the same cells, we used acetyl-β-methylcholine (MCh) (250 μM), which is known to decrease sIPSC activity through action on metabotropic cholinergic receptors on F2 terminals (3). Application of MCh (250 μM, 1.5 min) suppressed sIPSC activity to 53 ± 2.4% (n = 29) and to 43.6 ± 2.6% (n = 31) of the baseline value in TRPC4$^{+/+}$ (Fig. 3 *A* and *F*) and TRPC4$^{-/-}$ (Fig. 3 *D* and *F*) cells, respectively. Furthermore, responses to DHPG (100 μM) were not significantly different in TRPC4$^{+/+}$ (2,678.8 ± 928.1%, n = 7) and TRPC4$^{-/-}$ (2,577.6 ± 253.6%, n = 10) cells (Fig. 3*F*). Taken together, the data indicate that F2 terminals are functional in the knockout mice and that 5-HT responses are critically dependent on the TRPC4 protein. The preservation of responses to DHPG in TRPC4$^{-/-}$ mice supports the view of a functional PLC system and a divergence of downstream mechanisms on 5-HT$_2$ receptor and group I mGluR-mediated PLC activation, most likely the contribution and lack of TRPC4, respectively. Furthermore, depolarizing responses to 5-HT mediated via 5-HT$_2$ receptors in neurons of the reticular thalamic nucleus (30) were indistinguishable in TRPC4$^{+/+}$ (n = 6) and TRPC4$^{-/-}$ (n = 6) mice, evidence against a global abnormality of 5-HT$_2$ receptor function in TRPC4-deficient mice (Fig. 8, which is published as supporting information on the PNAS web site).
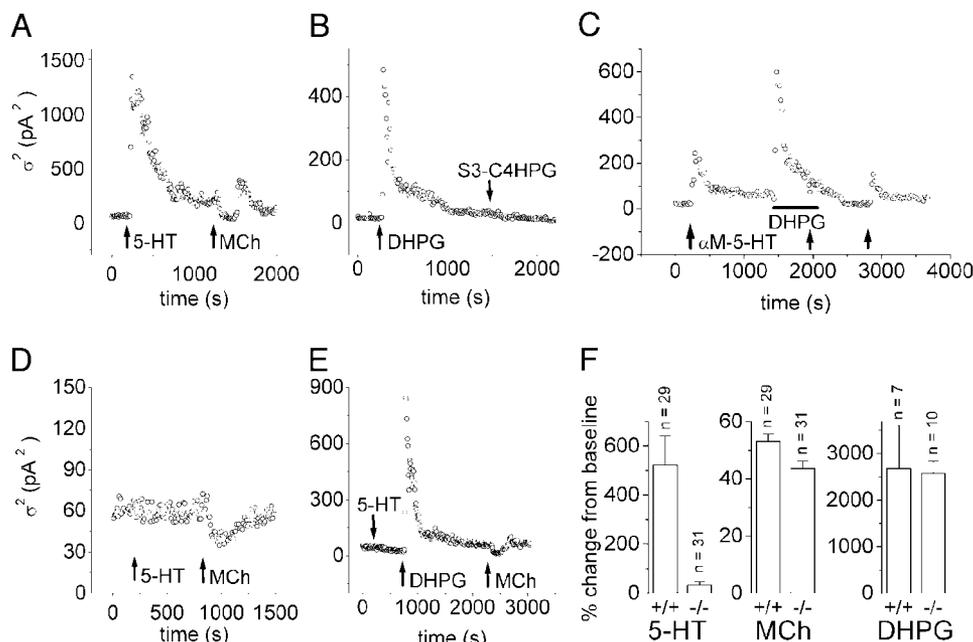
Fig. 3. Contribution of TRPC4 proteins to 5-HT-mediated GABA release from F2 terminals. (*A* and *D*) Changes in membrane current variance on bath-application of 5-HT (100 μM, 1.5 min) and acetyl-β-methylcholine (MCh) (250 μM, 1.5 min) in relay cells of wild-type (TRPC4$^{+/+}$, *A*) and TRPC4 knockout (TRPC4$^{-/-}$, *D*) mice. (*B*) Changes in membrane current variance on bath-application of mGluR agonists DHPG (100 μM) and (*S*)-3-carboxy-4-hydroxyphenylglycine (S3-C4HPG) (250 μM) in TRPC4$^{+/+}$ mice. (*C*) Occlusion of αM-5-HT (100 μM) induced an increase in IPSC activity during the nearly maximal action of DHPG (100 μM) in TRPC4$^{+/+}$ mice. (*E*) Persistence of DHPG-induced increase in IPSC activity in TRPC4$^{-/-}$ mice. (*F*) Summary of the effects of 5-HT, MCh, and DHPG, normalized to basal membrane current variance before application of substances, for wild-type (TRPC4$^{+/+}$) and TRPC4-deficient (TRPC4$^{-/-}$) mice, respectively. All recordings were obtained in the presence of TTX (1 μM). Error bars show SEM.

Electron microscopy did not indicate any anatomical abnormalities in various brain areas, including F2 terminals in the LGNd, in TRPC4$^{-/-}$ mice (data not shown). Although available antibodies recognize both variants of TRPC4 present in mice, TRPC4 and TRPC4$_{\Delta 781-864}$, in immunoblots of mouse brain microsomal proteins, anatomical corroboration of the existence of TRPC4 proteins in F2 terminals could not be obtained in the present study because of the limited applicability of the antibodies for immunohistochemistry. To obtain more direct evidence of the coexpression of TRPC4 and serotonergic receptors in the GABAergic interneurons, we studied mRNA expression in interneurons that had been isolated and identified from the rat LGNd (8). As illustrated in Fig. 4, the isolated neurons coexpressed TRPC4 and 5-HT receptors of the 2A and 2C subtypes, as well as glutamic acid decarboxylase (GAD67) and calbindin-28K, thereby further indicating that they represented GABAergic interneurons of the LGNd (31).

Discussion

The results of the present study demonstrate that the release of GABA from interneuronal dendrites onto thalamic relay cells is under the control of receptor-mediated Ca^{2+}-influx and that TRPC4 proteins are critically involved in these Ca^{2+}-influx pathways, thereby ascribing a functional role of TRP channels to the release of transmitters from dendrites. These pathways involve metabotropic serotonin but not group I mGluRs, thereby contrasting with the coupling of postsynaptic mGluRs to TRP-like conductances in cultured hippocampal CA3 neurons (32) and cerebellar Purkinje cells (33). The intracellular pathways that couple the 5-HT$_2$ receptors to the Ca^{2+}-influx mechanism seem to depend on the PLC system, although the present data do not allow a firm conclusion on the contribution of inositol trisphosphate or related mechanisms that couple the receptors to the cation channels in the plasma membrane. Overexpressed TRPC4 in chromaffin cells and PC12 cells (34) and heteromeric
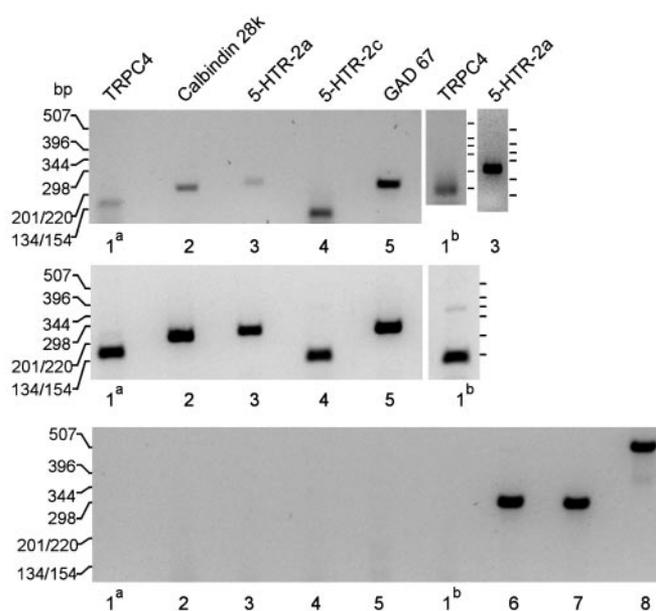
Fig. 4. RNA expression analysis in isolated LGNd interneurons. Amplification of reverse-transcribed mRNA of TRPC4 (lanes 1[a] and 1[b]), calbindin-28K (lane 2), 5-HT receptor 2a (lane 3), 5-HT receptor 2c (lane 4), and GAD67 (lane 5) from interneurons acutely isolated from rat LGNd slices (10 interneurons per reaction, *Top*) or from brain (poly)A$^+$ RNA (*Middle*), respectively. Primers (Table 1) were derived from different exons of a given gene, and no amplification products were obtained with the same amplification protocol in the absence of cells (data not shown) or when genomic DNA was used as a template (*Bottom*), whereas control amplifications using primer pairs located within a single exon yielded the expected DNA fragments from genomic DNA (lanes 6–8; Table 2). The number of experiments was 2–3. The identities of all amplified DNA fragments were confirmed by the sequencing of both strands.

NEUROSCIENCE

TRPC1/TRPC5 and TRPC1/TRPC4 overexpressed in HEK293 cells (29) yield channels that are activated by Gq-coupled receptors through PLCβ but not by protocols known to deplete intracellular Ca^{2+} stores. The specific effector molecules directly responsible for channel activation are unknown. In addition, the biophysical properties of overexpressed heteromeric TRPC1/TRPC5 and TRPC1/TRPC4 were reported to be distinct from those of the overexpressed TRPC homomers (29), whereas endogenously expressed TRPC4 contributes to store-operated channel activity in mouse endothelial cells (6) and in bovine adrenal cortex cells (35). The reasons for these different observations are unknown at present, but assembly of TRPC4, TRPC1, and currently unidentified additional proteins might be responsible for the diversity of TRPC4 channel activity and activation. In view of this presumed complex heteromeric organization of native TRP channels (28, 29), it is not to be expected that TRPC4 subunits represent the exclusive element in the regulation of dendritic GABA release, which in turn corresponds to the findings that responsiveness was drastically reduced, but not fully abolished, in TRPC4-deficient mice.

The results of the present study indicate a mechanism by which the ascending serotonergic brainstem system is capable of controlling sensory signal processing in the thalamus, depending on the sleep/waking cycle (4, 5). It is known that the firing of serotonergic neurons in the dorsal raphé nucleus is state-dependent, with fastest rates occurring during wakefulness and vigilance (36), and that visual contrast sensitivity in thalamic neurons increases during periods of increased arousal (37). Furthermore, the processing of visual contrast information in the thalamus heavily depends on local GABAergic interactions mediated via F2 terminals (1), and interactions have been particularly observed between GABAergic and serotonergic influences (38). The data of the present study may mechanistically link these observations, in that the increase in activity of the serotonergic system will promote the release of GABA from interneuronal dendrites, thereby leading to an increase in local GABAergic inhibition and a related increase in contrast processing. Through regulation of the F2 output, the serotonergic system thus may act in concert with the ascending cholinergic brainstem and descending glutamatergic fibers from the cortex (2, 3) to achieve a finely tuned balance of local information processing in the LGNd depending on the needs of a particular behavioral state.

1. Sherman, S. M. & Guillery, R. W. (1996) *J. Neurophysiol.* **76,** 1367–1395.
2. Cox, C. L., Zhou, Q. & Sherman, M. (1998) *Nature* **394,** 478–482.
3. Cox, C. L. & Sherman, M. (2000) *Neuron* **27,** 597–610.
4. Steriade, M. & McCarley, R. W. (1990) *Brainstem Control of Wakefulness and Sleep* (Plenum, New York).
5. McCormick, D. A. & Bal, T. (1997) *Ann. Rev. Neurosci.* **20,** 185–215.
6. Freichel, M., Suh, S. H., Pfeifer, A., Schweig, U., Trost, C., Weissgerber, P., Biel, M., Philipp, S., Freise, D., Droogmans, G., Hofmann, F., Flockerzi, V. & Nilius, B. (2001) *Nat. Cell Biol.* **3,** 121–127.
7. Szinyei, C., Stork, O. & Pape, H. C. (2003) *J. Neurosci.* **23,** 2549–2556.
8. Pape, H. C., Budde, T., Mager, R. & Kisvárday, Z. F. (1994) *J. Physiol. (Paris)* **478,** 403–422.
9. Ottersen, O. P. & Storm-Mathisen, J. (1984) *Anat. Embryol.* **170,** 197–207.
10. Grossman, A., Lieberman, A. R. & Webster, K. E. (1973) *J. Comp. Neurol.* **150,** 441–466.
11. Kriebel, R. M. (1975) *J. Comp. Neurol.* **159,** 45–67.
12. Hoyer, D. & Martin, G. (1997) *Neuropharmacology* **36,** 419–428.
13. Powis, G., Seewald, M. J., Gratas, C., Melder, D., Riebow, J. & Modest, E. J. (1992) *Cancer Res.* **52,** 2835–2840.
14. Llansola, M., Monfort, P. & Felipo, V. (2000) *J. Pharmacol. Exp. Therap.* **292,** 870–876.
15. Maruyama, T., Kanaji, T., Nakade, S., Kanno, T. & Mikoshiba, K. (1997) *J. Biochem.* **122,** 498–505.
16. Ma, H.-T., Patterson, R. L., van Rosum, D. B., Birnbaumer, L., Mikoshiba, K. & Gill, D. L. (2000) *Science* **287,** 1647–1651.
17. Prakriya, M. & Lewis, R. S. (2001) *J. Physiol.* **536,** 3–19.
18. Ma, H.-T., Venkatachalam, K., Li, H. S., Montell, C., Kurosaki, T., Patterson, R. L. & Gill, D. L. (2001) *J. Biol. Chem.* **276,** 18888–18896.
19. Budde, T., Sieg, F., Braunewell, K. H., Gundelfinger, E. D. & Pape, H. C. (2000) *Neuron* **26,** 483–492.
20. Daly, J. W. (2000) *J. Auton. Nerv. Syst.* **81,** 44–52.
21. Shi, D., Padgett, W. L. & Daly, J. W. (2003) *Cell. Mol. Neurobiol.* **23,** 331–347.
22. Putney, J. W. (1990) *Cell Calcium* **11,** 611–624.
23. Schaefer, M., Plant, T. D., Obukhov, A. G., Hofmann, T., Gudermann, T. & Schultz, G. (2000) *J. Biol. Chem.* **275,** 17517–17526.
24. Plant, T. D. & Schaefer, M. (2003) *Cell Calcium* **33,** 441–450.
25. Hofmann, T., Schaefer, M., Schultz, G. & Gudermann, T. (2000) *J. Mol. Med.* **78,** 14–25.
26. Clapham, D. E., Runnels, L. W. & Strübing, C. (2001) *Nat. Rev. Neurosci.* **2,** 387–396.
27. Montell, C., Birnbaumer, L. & Flockerzi, V. (2002) *Cell* **108,** 595–598.
28. Philipp, S., Hambrecht, J., Braslavski, L., Schroth, G., Freichel, M., Murakami, M., Cavalie, A. & Flockerzi, V. (1998) *EMBO J.* **17,** 4274–4282.
29. Strübing, C., Krapivinsky, G., Krapivinsky, L. & Clapham, D. E. (2001) *Neuron* **29,** 645–655.
30. McCormick, D. A. & Wang, Z. (1991) *J. Physiol.* **442,** 235–255.
31. Luth, H. J., Winkelmann, E. & Celio, M. R. (1993) *J. Hirnforsch.* **34,** 47–56.
32. Gee, C. E., Benquet, P. & Gerber, U. (2003) *J. Physiol.* **546,** 655–664.
33. Kim, S. J., Kim, Y. S., Yuan, J. P., Petralia, R. S., Worley, P. F. & Linden, D. J. (2003) *Nature* **426,** 285–291.
34. Obukhov, A. G. & Nowycky, M. C. (2002) *J. Biol. Chem.* **277,** 16172–16178.
35. Philipp, S., Trost, C., Warnat, J., Rautmann, J., Himmerkus, N., Schroth, G., Kretz, O., Nastainczyk, W., Cavalié, A., Hoth, M. & Flockerzi, V. (2000) *J. Biol. Chem.* **275,** 23965–23972.
36. McGinty, D. & Harper, R. (1976) *Brain Res.* **101,** 569–575.
37. Livingstone, M. S. & Hubel, D. H. (1981) *Nature* **291,** 554–561.
38. Funke, K. & Eysel, U. T. (1995) *Neuroreport* **6,** 474–476.